A COMPACT THERMIONIC RF INJECTOR WITH RF BUNCH COMPRESSION FED BY A QUADRUPOLE-FREE MODE LAUNCHER*

F. Toufexis†[1], V.A. Dolgashev, C. Limborg-Deprey, S.G. Tantawi, SLAC, Menlo Park, CA 94025
[1]Also at Department of Electrical Engineering, Stanford University, Stanford, CA 94305.

Abstract

We present a design for a compact X-Band RF thermionic injector consisting of two iris-loaded accelerator structures. Both structures are fed by a single quadrupole-free TM_{01} mode launcher. In the first structure the electron bunches are extracted from a thermionic cathode. The second structure creates an energy chirp in the bunch for its further ballistic compression. This injector can produce short electron bunches without the need for a magnetic bunch compressor. We are developing this injector as part of a linac-based 91.392 GHz RF power source, which further comprises a booster linac and a mm-wave decelerator structure that extracts 91.392 GHz RF power from the electron beam. This source will be used to power a short-period RF undulator with 1.75 mm period.

INTRODUCTION

We propose to build a 13.5 nm extreme ultra violet light source, based on a novel mm-wave undulator operating at 91.392 GHz [1, 2]. For this source we will reuse most of the existing SLAC X-Band (11.424 GHz) test accelerator infrastructure [3]. We will replace the existing photo-gun with a thermionic RF injector. This injector, which is the topic of this paper, consists of a thermionic RF gun, an accelerating structure, and a quadrupole-free TM_{01} mode launcher feeding both the gun and the accelerator structure. The electron bunches are accelerated in a booster linac downstream of the injector, and RF power at 91.392 GHz is extracted from the beam in a W-Band decelerator structure. This power is then fed into the RF undulator.

The mm-wave undulator is cavity that has a loaded quality factor of approximately 12,700 [1], which corresponds to a filling time of 22 ns. The undulator requires an input RF pulse length that is several times its filling time in order to reach its steady state fields. A decelerator structure at the W-Band has a loaded quality factor of only 1,700, which corresponds to a filling time of approximately 3 ns. Therefore, when driven by a single bunch, the RF pulse generated by a decelerator structure will not have sufficient length to fill the undulator. We therefore decided to develop a multibunch thermionic RF injector, in order to produce a W-Band RF pulse that is long enough to fill the undulator. Additionally we need bunches with a small 6-D emittance because we will compress them to a small fraction of the wavelength at 91.392 GHz and focus them transversely into the small aperture of the decelerator structure. We also considered DC injectors with subharmonic bunching. A high-voltage low emittance thermionic DC injector using a small CeB_6 cathode has been developed for a Free Electron Laser [4–6]; however, the fact that it requires a DC voltage of approximately 500 kV and a complex bunching system makes it large and expensive. A low voltage DC injector with subharmonic bunching cannot satisfy the small emittance requirement.

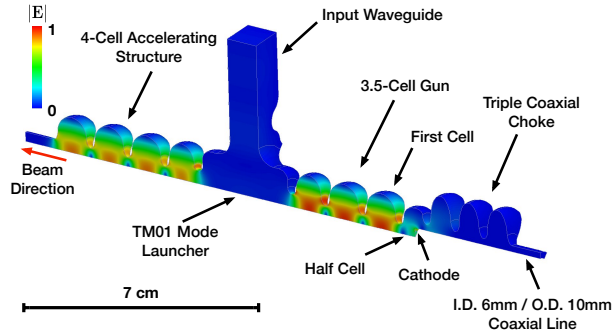

Figure 1: RF injector surface electric field on one eighth of the injector. The length of the structure shown is 18 cm.

Thermionic RF injectors at the S-Band have been employed in synchrotron light sources [7–10]. Most of these injectors used an alpha magnet for bunch compression. A higher frequency X-Band thermionic RF injector was built by the University of Tokyo for a Compton scattering source [11–17]. This injector also uses an alpha magnet for bunch compression. In this work we report a design for a compact X-Band thermionic RF injector with only RF bunch compression. We decided to use RF bunch compression instead of an alpha magnet due to space constraints in our system. A similar approach has been employed in a photo-gun [18–20].

DESIGN REQUIREMENTS

We designed the gun for a 70 MV m^{-1} peak electric field on the cathode and a 175 MV m^{-1} peak on-axis electric field of the other cells of the gun. The gun should produce appreciable current at cathode peak fields ranging from 60 MV m^{-1} to 90 MV m^{-1}. Due to beamline length constraints, the point of maximum bunch compression has to be within 0.6 m from the cathode. The following requirements must be met at that point: beam energy greater than 4 MeV, RMS bunch length σ_z less than 0.5 ps, transverse RMS bunch size σ_x, σ_y less than 1 mm, and bunch charge Q on the order of 7 pC. This charge corresponds to 80 mA of average current during the RF pulse. The RF power budget for the injector is 10 MW, and the RF pulse length is 250 ns.

* This project was funded by U.S. Department of Energy under Contract No. DE-AC02-76SF00515, and the National Science Foundation under Contract No. PHY-1415437.
† ftouf@stanford.edu

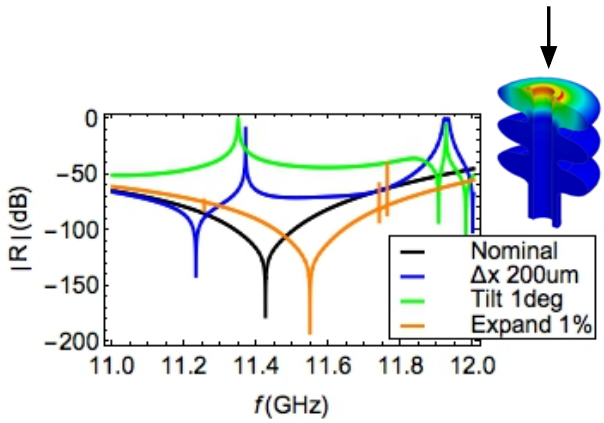

Figure 2: Triple choke reflection coefficient vs frequency for different perturbations of the cathode stem position.

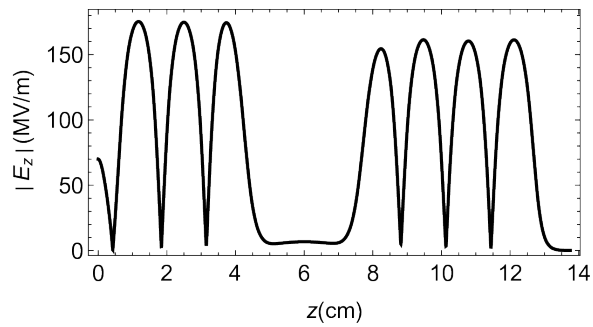

Figure 3: On-axis electric field amplitude profile for 8 MW of input power.

The cathode current density is conservatively assumed to be 10 A cm^{-2}.

RF DESIGN

The injector comprises a 3.5-cell thermionic RF gun, a 4-cell accelerating structure, and a quadrupole free mode launcher feeding both structures through the overmoded beam pipe. Figure 1 shows the circuit configuration and the surface electric field on one eighth of the injector. We plan to use a commercial 0.134 inch diameter flat face dispenser cathode. The cathode is mounted on a 6 mm diameter cathode stem. The gap between the cathode stem and the RF circuit of the gun is chosen to be 2 mm in order to reduce the possibility of RF breakdowns. The cathode half cell is formed using coaxial chokes with a 10 mm inner diameter. The cathode stem forms a coaxial line. Potential misalignment of the cathode stem could couple power to the TE_{11} in that coaxial line and result in power leakage. Therefore the dimensions of the coaxial line were chosen such that the TE_{11} cutoff frequency (11.9281 GHz) is above the operating frequency 11.424 GHz.

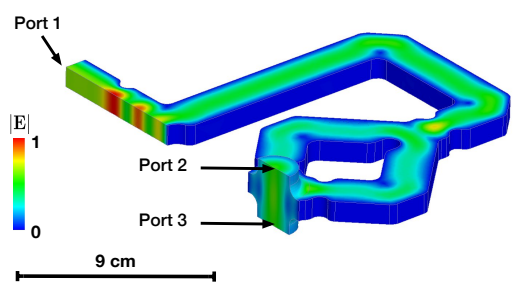

Figure 4: Quadrupole-free mode launcher half.

The shapes of the chokes and the accelerator cells are elliptical to reduce the probability of multipacting. We found that one or two chokes are not sufficient to stop RF leakage in the event of the cathode stem being misaligned. We therefore used three chokes in succession. Figure 2 shows the reflection coefficient of the triple choke when the stem is at its nominal position, when the stem is misplaced by 200 µm, when it is tilted by 1°, and when it is expanded by 1 % or 30 µm in radius. We found that the choke performance is most sensitive to cathode stem tilt.

The length of the half cell and of the first full cell of the gun – shown in Fig. 1 – were optimized for maximum *brightness times bunch charge* for 20 % of the bunch particles. This parameter was calculated using beam dynamics simulation in Astra [21]. For the optimization we run Astra without space charge. The beam dynamics simulation setup and post-processing are described in the next section. The resulting cell lengths were $0.5\lambda/2$ for the half cell, and $0.96\lambda/2$ for the first cell, where $\lambda = 2.62$ cm is the wavelength. The gun and the accelerating structure were then assembled with the mode launcher, as shown in Fig. 1. The distance between the structures was chosen using Astra. Figure 3 shows the on-axis electric field profile in the injector for 8 MW of input power. The peak surface electric field on the copper is 190 MV m^{-1}, and the peak surface magnetic field is 310 kA m^{-1}. From [22] the peak pulsed surface heating for 1 µs RF pulses is 41.3 °C, which is considered safe for copper [23].

Both the gun and the accelerator structure are fed through a TM_{01} mode launcher. This mode launcher comprises four rectangular TE_{10} to cylindrical TM_{01} power dividers and a power combining network. Figure 4 shows one half of

Table 1: Bunch Parameters at the Point of Maximum Compression $z = 65.78$ cm

	80 %	50 %	20 %	Spec.
$E\ (MeV)$	4.596	4.506	4.486	> 4
$Q\ (pC)$	6.322	3.900	1.485	~7
$I_{bunch}\ (A)$	4.895	41.14	56.43	
$B_n\ \left(\frac{A}{mm^2 mrad^2}\right)$	0.302	17.44	204.9	
$\sigma_x\ (\mu m)$	576.8	189.6	69.38	< 1000
$\sigma_y\ (\mu m)$	578.5	189.8	69.13	< 1000
$\sigma_z\ (fs)$	322.8	23.70	6.578	< 500
$\epsilon_{x,n}\ (mm \cdot mrad)$	5.674	2.167	0.747	
$\epsilon_{y,n}\ (mm \cdot mrad)$	5.707	2.176	0.737	
$\Delta E_{rms}\ (\%)$	3.498	1.012	0.4398	

ISBN 978-3-95450-182-3

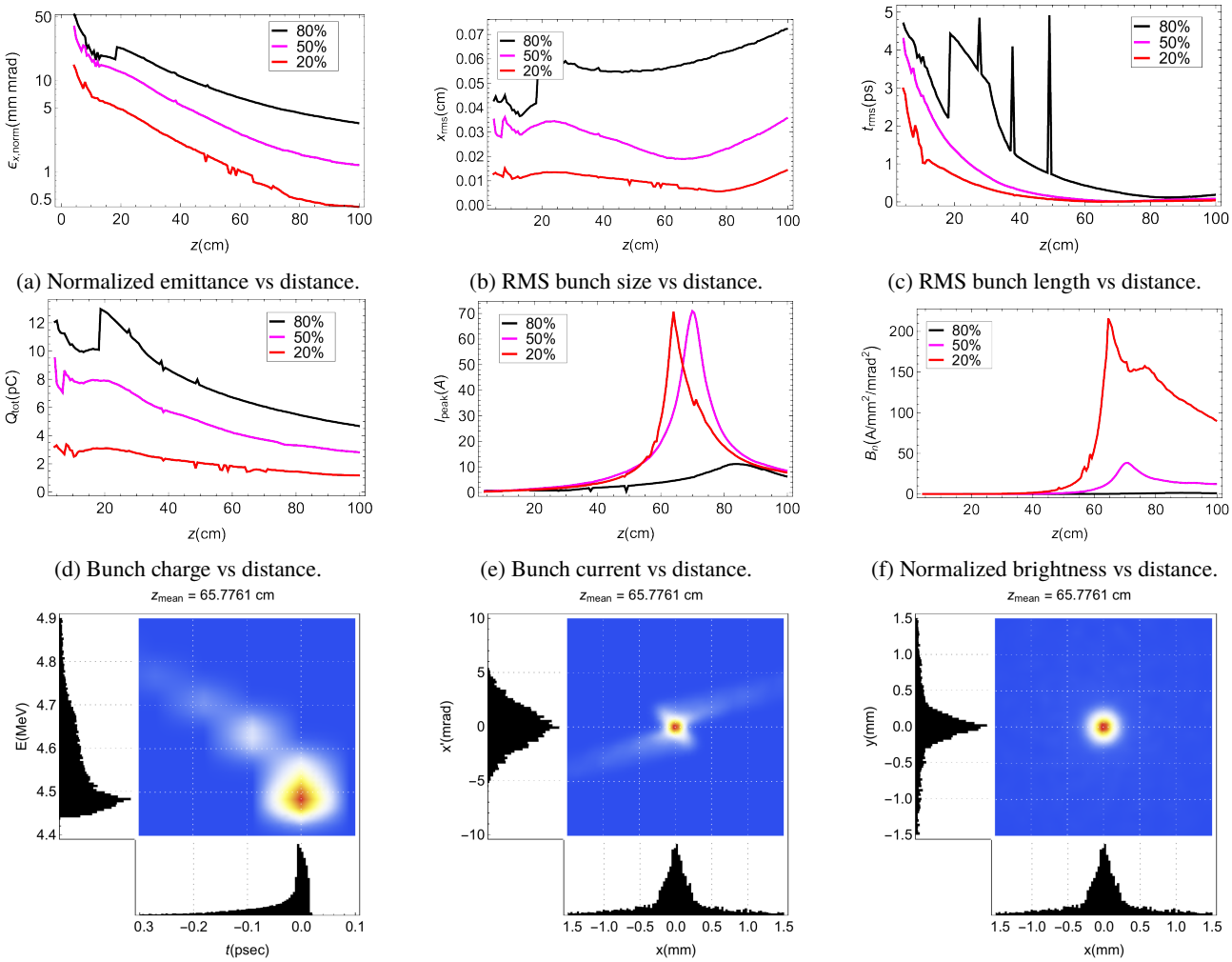

(a) Normalized emittance vs distance.

(b) RMS bunch size vs distance.

(c) RMS bunch length vs distance.

(d) Bunch charge vs distance.

(e) Bunch current vs distance.

(f) Normalized brightness vs distance.

(g) Long. phase space.

(h) Trans. phase space.

(i) Bunch cross-section.

Figure 5: Beam dynamics simulation results and phase space at the point of maximum compression.

the mode launcher. The four feeds around the cylindrical waveguide do not excite either dipole or quadrupole modes.

BEAM DYNAMICS

The beam input to Astra had a uniform in time distribution, equivalent to three RF buckets. We used the cylindrical space charge model in Astra. The beam pipe radius of the injector is 3 mm. Particles beyond that radius were discarded. To calculate single bunch parameters out of a multi-bunch phase space, the phase space was exported every 40 ps and was post-processed in Mathematica. Bunches were extracted from the phase space, and the parameters of the middle bunch were calculated for different fractions of the bunch. That fraction was calculated as follows: particles were iteratively filtered out of the particle array if they were more than two standard deviations away in energy or position from the particle array mean, until the number of remaining particles in the array was the required percentage of the original. The bunch current is calculated as $I_{bunch} = Q_{tot}/(4\sigma_z)$. The normalized brightness is defined as $B_n = 2I_{bunch}/\left(\epsilon_{x,n} \cdot \epsilon_{y,n}\right)$, where $\epsilon_{x,n}$ and $\epsilon_{y,n}$ are the normalized transverse emittance in the x and y directions. Figure 5 shows the bunch parameters versus distance from the cathode and phase space at z = 65.78 cm. Table 1 summarizes the bunch parameters at this z coordinate. As shown in Fig. 5d, the bunch charge drops with z because a significant part of the beam is diverging due to RF focusing and is lost in the beam pipe.

CONCLUSION

We have designed a compact X-Band thermionic RF injector, consisting of a 3.5-cell gun and a 4-cell accelerating structure, fed by a single TM_{01} mode launcher. This injector generates a train of electron bunches spaced 87.5 ps apart. The RF gun is designed to operate with 70 MV m^{-1} peak electric field on the cathode and approximately 175 MV m^{-1} peak on-axis field for the rest of the cells. The parameters of 80 % of the bunch are Q = 6.3 pC, $\sigma_{x/y}$ = 578 µm, σ_z = 323 fs, and $\epsilon_{x/y,n}$ = 5.7 mm mrad. The parameters of 20 % of the bunch are Q = 1.5 pC, $\sigma_{x/y}$ = 69 µm, σ_z = 6.6 fs, and $\epsilon_{x/y,n}$ = 0.75 mm mrad.

ISBN 978-3-95450-182-3

REFERENCES

[1] F. Toufexis and S. G. Tantawi, "A 1.75 mm Period RF-Driven Undulator," in *Proc. of International Particle Accelerator Conference (IPAC'17), Copenhagen, Denmark, May 14-19, 2017*. Geneva, Switzerland: JACoW, May 2017.

[2] F. Toufexis *et al.*, "Coupling and Polarization Control in a mm-wave Undulator," in *Proc. of International Particle Accelerator Conference (IPAC'17), Copenhagen, Denmark, May 14-19, 2017*. Geneva, Switzerland: JACoW, May 2017.

[3] C. Limborg-Deprey *et al.*, "Performance of a first generation X-band photoelectron rf gun," *Phys. Rev. Accel. Beams*, vol. 19, no. 5, p. 053401, May 2016.

[4] K. Togawa *et al.*, "CeB_6 electron gun for low-emittance injector," *Phys. Rev. ST Accel. Beams*, vol. 10, no. 2, p. 020703, Feb. 2007.

[5] T. Shintake *et al.*, "A compact free-electron laser for generating coherent radiation in the extreme ultraviolet region," *Nature Photonics*, vol. 2, no. 9, pp. 555–559, Jul. 2008.

[6] T. Shintake *et al.*, "Stable operation of a self-amplified spontaneous-emission free-electron laser in the extremely ultraviolet region," *Phys. Rev. ST Accel. Beams*, vol. 12, no. 7, p. 070701, Jul. 2009.

[7] M. Borland, "A High Brightness Thermionic Microwave Electron Gun," Ph.D. dissertation, Stanford University, Feb. 1991.

[8] S. Werin *et al.*, "A New 3 GHz RF-gun Structure for MAX-lab," 2000.

[9] A. Rajabi *et al.*, "Electron injector for Iranian Infrared Free Electron Laser," *Journal of Instrumentation*, vol. 11, no. 12, pp. P12 004–P12 004, 2016.

[10] A. Sadeghipanah *et al.*, "Bunch compression in low emittance pre-injection system of Iranian Light Source Facility," *Journal of Instrumentation*, vol. 11, no. 01, pp. P01 002–P01 002, 2016.

[11] M. Uesaka *et al.*, "X-band RF gun/linac for inverse Compton scattering hard X-ray source," in *Linear accelerator. Proceedings, 21st International Conference, Linac 2002, Gyeongju, South Korea, August 19-23, 2002*, 2002, pp. 626–628.

[12] A. Fukasawa *et al.*, "X-Band Thermionic Cathode RF Gun at UTNL," in *Proceedings of the 2005 Particle Accelerator Conference*, May 2005, pp. 1646–1648.

[13] K. Dobashi *et al.*, "Beam test of thermionic cathode X-band RF-gun and linac for monochromatic hard X-ray source," in *EPAC*, 2006, pp. 2319–2321.

[14] F. Sakamoto, M. Uesaka, and K. Dobashi, "X-band thermionic cathode RF gun and multi-beam Compton scattering monochromatic tunable X-ray source," *Journal of the Korean Physical Society*, vol. 49, no. 91, pp. 286–297, 2006.

[15] F. Sakamoto *et al.*, "Compton scattering monochromatic X-ray source based on X-band multi-bunch linac at the University of Tokyo," *Nuclear Instruments and Methods in Physics Research Section A: Accelerators, Spectrometers, Detectors and Associated Equipment*, vol. 608, no. 1, Supplement, pp. S36–S40, 2009.

[16] Y. Taniguchi *et al.*, "Upgrade of X-band thermionic cathode RF gun for Compton scattering X-ray source," *Nuclear Instruments and Methods in Physics Research Section A: Accelerators, Spectrometers, Detectors and Associated Equipment*, vol. 608, no. 1, Supplement, pp. S113–S115, 2009.

[17] T. Natsui *et al.*, "Beam Measurement of 11.424 GHz X-Band Linac for Compton Scattering X-ray Source," *AIP Conference Proceedings*, vol. 1299, no. 1, pp. 538–543, 2010.

[18] B. O'Shea *et al.*, "RF Design of the UCLA/INFN Hybrid SW/TW Photoinjector," *AIP Conference Proceedings*, vol. 877, no. 1, pp. 873–879, 2006.

[19] J. B. Rosenzweig *et al.*, "Design and applications of an X-band hybrid photoinjector," *Nuclear Instruments and Methods in Physics Research Section A: Accelerators, Spectrometers, Detectors and Associated Equipment*, vol. 657, no. 1, pp. 107–113, 2011.

[20] B. Spataro *et al.*, "RF properties of a X-band hybrid photoinjector," *Nuclear Instruments and Methods in Physics Research Section A: Accelerators, Spectrometers, Detectors and Associated Equipment*, vol. 657, no. 1, pp. 99–106, 2011.

[21] K. Floettmann, *ASTRA*, Deutsches Elektronen-Synchrotron, Hamburg, Germany. [Online]. Available: www.desy.de/~mpyflo/Astra_manual/Astra-Manual_V3.1.pdf

[22] V. A. Dolgashev, "High magnetic fields in couplers of X-band accelerating structures," in *Proceedings of the 2003 Particle Accelerator Conference*, May 2003, pp. 1267–1269 Vol.2.

[23] L. Laurent *et al.*, "Experimental study of rf pulsed heating," *Phys. Rev. ST Accel. Beams*, vol. 14, no. 4, p. 041001, Apr. 2011.

ISBN 978-3-95450-182-3